

Thesis book

Development and investigation of V2X  
communication-based control using  
Mixed-reality methods

*Author:*

**Tamás Ormándi**



Budapest University of Technology and Economics  
Department of Control for Transportation and Vehicle Systems

*Supervisor:*

**Dr. Balázs Varga**

October 6, 2025

# Introduction

V2X (Vehicle-to-Everything) communication marks a significant shift in intelligent transportation systems, enabling real-time data exchange between vehicles, infrastructure, pedestrians, and networks. With advancements in wireless technologies such as DSRC (Dedicated Short-Range Communications) [1] and C-V2X (Cellular V2X) [2], vehicles can now communicate with their surroundings to enhance road safety, reduce traffic congestion, and improve overall transportation efficiency. This connectivity allows for many applications ranging from collision avoidance and traffic signal optimization to cooperative driving and autonomous vehicle navigation.

A significant portion of research is dedicated to developing novel autonomous intersection control algorithms [3–5] for future implementation. However, challenges such as delays, interference [6], packet losses [7], signal attenuation [8], channel congestion [9] and hardware reliability in wireless communication are often overlooked, leaving a considerable research gap. These factors can degrade communication performance, directly impacting any control system that depends on data transmitted via wireless communication, which could lead to accidents or suboptimal performance. Algorithms are developed in various forms, including centralized [10–12] and distributed [13–15] solutions, each with its own advantages and limitations. The centralized control solution depends on an RSU or cloud server to gather, process, and distribute information, which can create a single point of failure for the entire system. Distributed solutions rely on each vehicle, ensuring single failures do not entirely stop intersection control. The effectiveness and safe operation of these algorithms heavily depend on rigorous testing and validation in corner cases, which can be both time-consuming and costly. Real-life testing of large-scale communication-based applications and algorithms is typically infeasible due to the low adoption rate of V2X-capable vehicles. Cybersecurity is another critical aspect of V2X communication, as the increasing connectivity of vehicles raises concerns about potential vulnerabilities and attacks on the system. Ensuring the security and privacy of V2X communication is essential to maintain trust in these technologies and their widespread adoption.

A major multi-lane intersection with heavy traffic volumes with centralized intersection control that can coordinate vehicle movement require a significant investment. However, simpler, more robust, and attack-resistant solutions are also needed for smaller

intersections, where centralized control is not feasible. By developing a distributed control algorithm, the reliance on a centralized system can be eliminated. This algorithm can be implemented directly on each vehicle, enabling them to communicate and make decisions based on shared information. This approach reduces system complexity while enhancing resilience against attacks and disruptions in wireless communication.

While numerous simulation solutions exist for modeling wireless communication, they tend to be slow due to their agent-based nature. Simulating a large number of vehicles in a microscopic environment can be time-consuming, making it impractical for testing large-scale V2X applications. Moreover, advanced testing methods like VIL (Vehicle-In-the-Loop) testing with mixed-reality integration are not feasible with conventional V2X communication simulations, as they require real-time performance. Achieving high-performance simulations with high accuracy requires the development of a novel V2X simulation method, that can fully utilize the capabilities of both microscopic (agent-based) and macroscopic (aggregated) solutions. In this work, a highly detailed co-simulation environment is utilized for algorithm development, analysis and the development of a new test framework with mixed-reality. A general architecture of this simulation and mixed-reality framework is presented in Fig. 1.

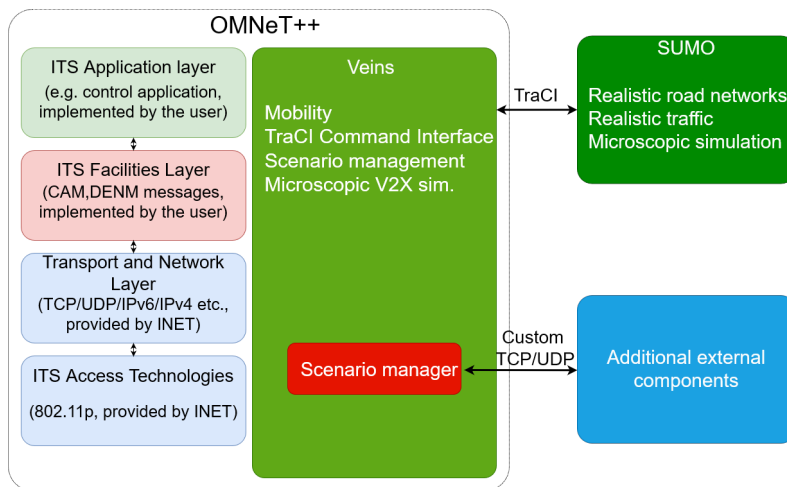


Figure 1: Co-simulation ecosystem.

OMNeT++ is employed as the main network simulator, incorporating the Veins and INET frameworks for communication layer modeling, and connected to SUMO to enable realistic traffic simulation.

By employing a real-time capable approach, V2X simulation can be integrated into a mixed-reality environment utilizing real vehicles and V2X hardware, enabling the testing of V2X communication-based control algorithms in a realistic setting. This integration allows researchers to assess algorithm performance in a controlled environment while maintaining a high level of realism for the tested vehicle. With the help of a new V2X simulation approach, the wireless communication of large-scale virtual traffic can be re-

---

alized utilizing a single V2X hardware. By incorporating additional models for signal propagation and fully leveraging V2X simulation, the accuracy of the mixed-reality test system can be significantly improved. Furthermore, using digital twin technology to account for the impact of distance between virtual and physical vehicles enhances realism even further.

# Contributions of the Thesis

## Thesis 1

### Thesis 1

I have developed a novel methodology for the sensitivity analysis of control solutions based on wireless communication, utilizing high-precision simulation. I demonstrated that state-of-the-art intersection control algorithms exhibit high sensitivity to communication delays and packet losses. The degradation of communication resulted in up to a 122% increase in average traffic speed, up to a 17% absolute deviation in road segment occupancy, as well as a significant rise in accident risk. Furthermore, I identified cybersecurity risks specific to individual algorithms, as well as delays stemming from computational performance limitations. In addition, I conducted an FMEA analysis for V2X-compatible autonomous vehicles and autonomous intersections.

Related publications: [A, B, C, D, J]

Various wireless communication-based algorithms for controlling autonomous intersections, both centralized and decentralized, with varying levels of complexity, have been examined in the literature. Their strengths and weaknesses were thoroughly examined and presented, highlighting both the advantages they offer and the potential limitations or challenges they may present in real-world applications. However, most of these studies fail to account for the significant impacts and uncertainties inherent in wireless communication (see Table 1).

In this thesis, algorithms were developed within a high-precision simulation environment that considers the effects across all communication layers, from the physical layer (radio signal propagation, interference) to the application layer (the control algorithm itself). The simulation framework also incorporates details such as the serialization and deserialization of standard packets providing highly detailed delays.

The implemented algorithms are:

1. FCFS (First Come First Served), which allows only the nearest vehicle to enter the intersection.

Table 1: A comparison table for state of the art solutions and their problems. ✓ means the problem is present for the algorithm type. Implemented algorithms are highlighted at algorithm types in brackets.

| Algorithm type                                  | Problems          |                |                                |                             |                                    |                       |
|---|-------------------|----------------|--------------------------------|-----------------------------|------------------------------------|-----------------------|
|   | Full control loss | Ghost vehicles | High penetration rate required | Strict trajectory following | Highly automated vehicles required | Computationally heavy |
| Centralized (FCFS, Virtual Traffic light, MCTS) | ✓                 | ✓              | ✓                              | -                           | ✓                                  | ✓                     |
| Decentralized (CAM-based)                       | X                 | ✓              | ✓                              | -                           | ✓                                  | X                     |
| Spatiotemporal solutions (Grid-based)           | -                 | ✓              | ✓                              | ✓                           | ✓                                  | ✓                     |
| Trajectory planning                             | -                 | ✓              | ✓                              | ✓                           | ✓                                  | X                     |

2. The CAM-based algorithm, which enforces the priority-to-the-right rule.
3. The Virtual Traffic Light algorithm, which implements traffic light control solely through V2X messages
4. The MCTS (Monte Carlo Tree Search) algorithm, which adjusts vehicle speeds for seamless and secure flow through the intersection by only affecting vehicle speeds searching for the best order.
5. The grid-based algorithm, which scans the discretized intersection and reserves paths for approaching vehicles.

Corner case scenarios with high and low traffic densities were created to demonstrate the impact of these factors on algorithm performance, analyzing key traffic flow parameters such as average vehicle speed (see Table 2), edge occupancies (see Table 3), and data-related packet drops. The corner case scenarios included multiple instances with varying radio noise levels, which impacted both the timing and quantity of received data. All noise levels were applied across all traffic densities, resulting in a large number of simulations. Additionally, the algorithms were evaluated against a range of cyberattacks relevant to their operation, which could potentially lead to significant performance degradation or even accidents.

In addition to the detailed examination of the algorithms, a Failure Mode and Effects Analysis (FMEA) was presented for autonomous intersections and V2X-compatible autonomous vehicles, which took into account not only potential software failures but also hardware-related and environmental impacts.

The main findings of the analysis were that the algorithms exhibit significant sensitivity to neglected communication factors (e.g., data loss, delays, noise), which negatively affect the safety and throughput of the intersection. The findings highlight the importance of considering communication factors in the design and evaluation of intersection control algorithms, as they can significantly impact their performance and safety which is especially important in safety critical applications. Algorithms that rely on multiple parameters that require fine-tuning and complex calculations are more sensitive to communication factors, while simpler algorithms are more robust. Each new algorithm should be analyzed in various corner case scenarios to ensure they can handle the effects of communication degradation or cyberattacks. The control algorithms must guarantee safety and collision avoidance even in the presence of communication failures whether it is a centralized or a decentralized case. Redundancy with fallback to sensor-based solutions is also recommended.

Table 2: Summary of the algorithms achieved average vehicle speed during all simulation cases. Values are in m/s. High means the high traffic flow, and low is for the lower traffic flow cases. Best performing algorithm is grayed out.

| Algorithm             | High - normal | High - noise | High - strong noise | Low - normal | Low - noise | Low - strong noise |
|-----------------------|---------------|--------------|---------------------|--------------|-------------|--------------------|
| FCFS                  | 1.7084        | 0.8313       | 0.4414              | 0.5878       | 0.9841      | 0.7322             |
| CAM-based             | 2.9763        | 3.1546       | 3.1687              | 12.1183      | 12.2631     | 12.2662            |
| Virtual Traffic Light | 1.5119        | 1.4922       | 1.4885              | 2.1881       | 2.0531      | 2.037              |
| MCTS                  | 5.4411        | 6.4223       | 6.1848              | 8.9163       | 8.8118      | 11.0629            |
| Grid-based            | 2.1256        | 2.6378       | 2.14                | 2.017        | 2.3466      | 1.5473             |

Table 3: Summary of mean occupancy data. The table contains the average of the four edges occupancy values. Differences are regarding the cases (normal, noise, and strong noise). Best performer is highlighted.

| Algorithm and case                 | High traffic | Difference | Low Traffic | Difference |
|------------------------------------|--------------|------------|-------------|------------|
| FCFS normal                        | 57.52%       | -          | 58.87%      | -          |
| FCFS noise                         | 59.66%       | -2.14%     | 51.11%      | 7.76%      |
| FCFS strong noise                  | 62.03%       | -2.37%     | 55.67%      | -4.56%     |
| CAM-based normal                   | 41.19%       | -          | 4.55%       | -          |
| CAM-based noise                    | 39.86%       | 1.33%      | 4.48%       | 0.07%      |
| CAM-based strong noise             | 39.21%       | 0.65%      | 4.49%       | -0.01%     |
| Virtual Traffic Light normal       | 58.02%       | -          | 44.72%      | -          |
| Virtual Traffic Light noise        | 58.17%       | -0.15%     | 46.96%      | -2.24%     |
| Virtual Traffic Light strong noise | 58.22%       | -0.05%     | 47.22%      | -0.26%     |
| MCTS normal                        | 16.71%       | -          | 5.3%        | -          |
| MCTS noise                         | 13.51%       | 3.2%       | 4.74%       | 0.56%      |
| MCTS strong noise                  | 14.45%       | -0.94%     | 3.96%       | 0.78%      |
| Grid-based normal                  | 54.61%       | -          | 43.85%      | -          |
| Grid-based noise                   | 50.76%       | 3.85%      | 37.47%      | 6.38%      |
| Grid-based strong noise            | 54.39%       | -3.63%     | 51.76%      | -14.29%    |

---

## Thesis 2

### Thesis 2

I have developed a distributed intersection control algorithm based on V2X communication, aiming to improve both the throughput and safety of intersections. I have analyzed the performance of the algorithm using high-precision simulation under varying levels of radio noise and packet loss. According to the results, the algorithm reduced waiting time by 29% and decreased the variance of travel time within the network by 99% compared to the baseline case of an uncontrolled four-way intersection. I have also evaluated the algorithm from a cybersecurity perspective, and it remained robust against both communication errors and cyberattacks. In addition, I have tested the algorithm with real vehicles and V2X hardware.

Related publications: [A, B, J]

A straightforward, logic-based decentralized (without the need of centralized solutions and other signalization infrastructure) intersection control algorithm was developed and implemented within the V2X simulation framework. This algorithm operates solely on data coming from CAM (Cooperative Awareness Messages) exchanged between vehicles, and it does not require any additional information to be distributed among the vehicles. The logic behind this algorithm is designed to enforce a basic right of way rule, giving priority to vehicles approaching from the right side of the intersection. By relying exclusively on these minimal communication messages, the algorithm offers a simple yet effective solution for intersection management in a decentralized V2X environment.

The algorithm has a very low computational demand as it only calculates the distance of vehicles from the center of the intersection by using the Haversine formula:

$$A = \sin^2 \left( \frac{\Phi_2 - \Phi_1}{2} \right) \quad (1)$$

$$B = \cos(\Phi_1) \cos(\Phi_2) \sin^2 \left( \frac{\lambda_2 - \lambda_1}{2} \right) \quad (2)$$

$$d = 2r \arcsin \left( \sqrt{A + B} \right) \quad (3)$$

where  $d$  is the distance of the vehicle from the intersection in km,  $\Phi_1, \Phi_2$  are the latitude of point 1 and point 2 in radians,  $\lambda_1, \lambda_2$  are the longitude of point 1 and 2 in radians and  $r$  is the radius of Earth in km.

The direction of incoming vehicles is calculated by the relative heading:

$$H_{\text{relative}} = H_s - H_r \quad (4)$$

---

If  $H_{\text{relative}} < 0$ , then  $H_{\text{relative}} = H_{\text{relative}} + 360$

$$\text{direction} = \begin{cases} \text{same direction,} & 0 \leq H_{\text{relative}} < 45 \text{ or } 315 \leq H_{\text{relative}} < 360 \\ \text{from left side,} & 45 \leq H_{\text{relative}} < 135 \\ \text{from front,} & 135 \leq H_{\text{relative}} < 225 \\ \text{from right side,} & 225 \leq H_{\text{relative}} < 315 \end{cases} \quad (5)$$

Additionally, the algorithm calculates the arrival times for vehicles extended with a safety time window by using the vehicle's distance from the intersection and its actual speed, and makes a control decision based on that.

The algorithm depends on a single incoming message, providing a robust solution against interference and packet loss. The algorithm was tested in a high-precision simulation environment, where the impact of communication factors on the performance of the algorithm was analyzed. The results showed that the algorithm is capable of reducing the variance of individual travel times of vehicles by 99.43%. As a result of the control, each vehicle spends an average of 6.8 seconds less at the intersection, representing a relative reduction of 29.16%, under unsaturated traffic conditions.

The algorithm was also tested against cyberattacks by introducing fake data from a vehicle. Despite the active attack, the algorithm successfully prevented collisions. The algorithm was also analysed with additional radio interference and found to be resilient against packet losses. In *Thesis 1* (represented as the CAM-based algorithm), it was compared with other algorithms from the literature and found to be the top performer.

The developed algorithm was also realized with real vehicles and Cohda Wireless MK5 OBUs, demonstrated as a driver assistance solution with HMI (human-machine interface) support. To demonstrate the algorithm's practical implementability and its potential integration into an ADAS system.

---

## Thesis 3

### Thesis 3

I have developed a novel mesoscopic V2X simulation method that reduced the average duration of simulation steps by 96% compared to classical microscopic V2X simulation. With this new approach, real-time V2X simulation becomes achievable, which is essential for mixed reality-based simulations. The core of the solution lies in aggregating the frequency of messages generated by simulated vehicle traffic into a single node using a neural function approximator. The method reproduced the number of lost and received packets with an error of at most 10%. I have also demonstrated correlations between the frequency of CAMs and traffic dynamics. Based on these findings, the average vehicle count exhibited a moderate linear and strong positive monotonic correlation, which proved to be statistically significant. By contrast, average speed, average acceleration, and average heading deviation showed negligible correlations.

Related publications: [E, F, J]

Based on the results of *Thesis 1*, the need of a novel V2X simulation method was identified, which can be used to elevate simulation speed while keeping accuracy and open the way for new testing and validation methods. The complexity of agent-based V2X simulation with complex applications is  $\mathcal{O}(2^n)$  exponential. A mesoscopic V2X simulation method was developed to significantly accelerate wireless communication simulation compared to the state of the art. It is capable of simulating a large number of vehicles with high accuracy while maintaining real-time performance.

This is achieved by aggregating the radio messages generated by the simulated traffic, which reduces the computational load on the system in a single "Mesoscopic node". The area around the vehicle under test (EGO) is discretized into three distinct zones as follows:

1. Microscopic area: Where each vehicle is included in the simulation and their communication is simulated on the microscopic level. This ensures the high level of details of the immediate surroundings of the EGO vehicle.
2. Mesoscopic area: Which extends the microscopic area further to cover the entire communication range around the EGO vehicle. In this area, the entire traffic's communication is aggregated into mesoscopic nodes. The role of the mesoscopic zone is to accurately represent the communication of distant traffic while ensuring high simulation performance levels.
3. Macroscopic area: Where network nodes are outside of communication range and

are excluded from the simulation. The effect of these vehicles regarding their communications can be neglected, without affecting the tested EGO vehicle.

The mesoscopic approach is depicted in Fig. 2.

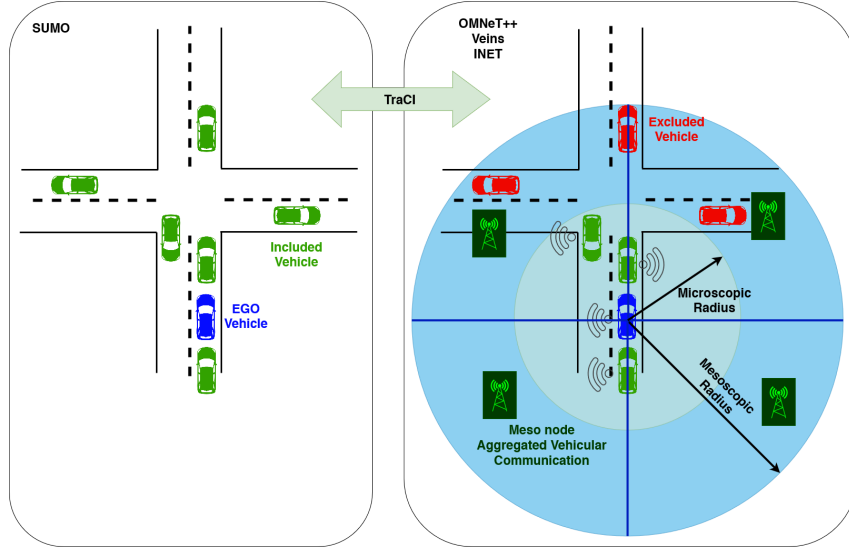


Figure 2: Mesoscopic V2X simulation approach.

The primary objective of the mesoscopic simulation is to aggregate the communication of the entire traffic within a chosen area into a single node, significantly reducing the number of simulated communicating nodes. The mesoscopic node (or meso node) predicts the number of messages that would be sent by the agents in its area using a neural network function approximator and transmits them at the required frequency for a 5-second time window.

The function approximator was trained using randomly sampled simulation data from multiple road networks with varying traffic conditions. Vehicles were bound only to the trained mesoscopic circular section by the following rules:

$$d = \sqrt{(d_x)^2 + (d_y)^2} \quad (6)$$

$$\Theta = \arctan(dy, dx) \cdot (180/\pi) \quad (7)$$

Eq. 6 calculates the distance between the vehicle and the center of the circular section.  $d_x = x - x_{center}$  and  $d_y = y - y_{center}$  are measuring the distances between the  $x$  and  $y$  coordinates of the vehicles and the circular section's center points. In Eq. 7, the polar angle is calculated. The result of the insertion check can be done with Eq. 8.

$$\text{result} = \begin{cases} \text{True, if} & [(\Theta > \alpha_{start}) \wedge (\Theta < \alpha_{end})] \wedge [(d < r_{sector}) \wedge (d > r_{micro})] \\ \text{False} & \text{otherwise} \end{cases} \quad (8)$$

where  $\alpha_{start}$  is the starting angle of the circular section,  $\alpha_{end}$  is the end angle of the circular section,  $r_{sector}$  is the radius of the mesoscopic circular sector and  $r_{micro}$  is the radius of the microscopic circle.

To aggregate the section’s traffic, the mesoscopic node computes the following moving averages for its own section from the past 5 seconds:

1. Average vehicle speed
2. Average vehicle heading
3. Average difference of the vehicle headings
4. Average acceleration of vehicles
5. Average number of vehicles

These traffic data are closely related to the CAM generation [16] and are used as inputs for the function approximator.

To compensate the missing packet collisions, the transmitter power of the mesoscopic node is adjusted after the 5 second period. The mesoscopic node uses the following equation to calculate the required transmission power:

$$P_T = N_v * \lambda \tag{9}$$

where  $P_T$  is the transmitter power in  $[W]$ ,  $N_v$  is the number of average vehicles in the mesoscopic node’s section and  $\lambda$  is a scenario specific constant found empirically for the desired scenario.

Simulation performance also depends on the simulation step size, which in turn influences the transmission frequency of the mesoscopic node. The greater the number of messages the node has to send, the smaller the time step the timer must use. With a smaller time step, the simulation performance will degrade. This necessitates modifying the time step during the simulation and keeping it at the highest possible level. A dynamic timer was implemented to maximize simulation performance and speed.

The correlation between CAM generation parameters and transmission frequency was presented (see Table 4).

Table 4: Correlation between parameters and the CAM sending frequency.

| Parameter                  | Correlation |          |                |
|----------------------------|-------------|----------|----------------|
|                            | Pearson     | Spearman | p-value        |
| Average number of vehicles | 0.46        | 0.83     | 0              |
| Average speed              | 0.01        | 0.16     | $4.76e^{-110}$ |
| Average acceleration       | -0.01       | -0.03    | 0.0001         |
| Average heading difference | -0.02       | -0.01    | 0.46           |

The Pearson Correlation (0.46) indicated that a moderate positive linear relationship is present between the variables in case of the average number of vehicles. The Spearman correlation showed, that a strong monotonic relationship is present between the average number of vehicles and the CAM sending frequency. The p-value of 0 indicates that the correlation is statistically significant. Other parameters showed no significant correlation.

The novel mesoscopic V2X simulation approach was tested on two different road networks (Ingolstadt and Gyöngyös, modeled in SUMO) and with realistic traffic. The results showed, that the presented solution is capable of simulating a large number of vehicles with high accuracy while maintaining real-time performance, achieving an average of 95.89% reduction in the time step duration. Accuracy was preserved, with the difference in packet drops and received packets remaining under 10% (see Table 5).

Table 5: Summary of the simulation results with the corresponding  $\lambda$  values.

| Scenario               | Results                    |                           |                 |           |
|------------------------|----------------------------|---------------------------|-----------------|-----------|
|                        | Packet drops (microscopic) | Packet drops (mesoscopic) | Relative change | $\lambda$ |
| Ingolstadt             | 5568                       | 5012                      | -9.99%          | 3.1       |
| Ingolstadt alternative | 310                        | 309                       | -0.32%          | 0.0035    |
| Gyöngyös               | 995                        | 1018                      | 2.31%           | 0.04      |
| Gyöngyös alternative   | 300                        | 313                       | 4.33%           | 1.35      |

---

## Thesis 4

### Thesis 4

I have developed a mixed reality-based testing system that enables the communication of virtual vehicles in the physical space through mesoscopic V2X simulation. Within the system, I applied digital twin technology, allowing real vehicles to participate in both traffic and communication simulations in real time. By employing inverse propagation models, I brought the average signal strength of communication between real and virtual vehicles up to 58% closer, thereby capturing the physical impact of distance between real and virtual vehicles. Using software-defined radio, I generated real radio interference based on simulation data, which resulted in up to 30% packet loss in real communication, thus representing the interference occurring in real-world environments.

Related publications: [E, F, G, H, I, J]

Expanding on the simulation solution developed in *Thesis 3*, a new V2X-based mixed-reality test framework was created. This framework enables the testing of V2X-based control algorithms in a mixed-reality environment, allowing real vehicles to interact with virtual traffic. It employs the mesoscopic V2X simulation method to represent the communication of virtual vehicles in the physical domain. The framework can simulate a large number of vehicles with high accuracy while maintaining real-time performance.

The mesoscopic node of the simulation was interconnected with an automotive V2X hardware (Cohda Wireless MK5 RSU). As a proof of concept measurement, a static mesoscopic node was created (the RSU) which was able to send the messages predicted by the mesoscopic simulation. Two EGO vehicles were equipped with Cohda Wireless MK5 OBUs, which were able to receive the messages sent by the mesoscopic node. This measurement showed the mixed-reality capabilities of the proposed system, that can realize the communication of virtual vehicles in the physical domain.

The system was then further extended by integrating a digital twin system based on V2X communication, enabling real vehicles to move in real-time both in the traffic simulator and the communication simulation. The digital twin was then utilized to realize the effect of distance between virtual and real vehicles by regulating transmission power using an inverse fading model.

The steps to calculate the required transmitter power for modeling signal propagation between real and virtual vehicles using V2X hardware - by inverting the Rician fading model [17] - are as follows:

$P_{rx}$  is converted from the input which is the output of the CAM message simulation between the probe node and the digital twin of the EGO vehicle in OMNeT++.  $R_r$

---

depends on  $K_{rician}$  and random variables  $x$  and  $y$  drawn from a normal distribution:

$$R_r = \frac{1}{2(K_{rician} + 1)} \left[ (x_{rician} + \sqrt{2K_{rician}})^2 + y_{rician}^2 \right] \quad (10)$$

$$x_{rician}, y_{rician} \sim \mathcal{N}(0, 1) \quad (11)$$

$L_{fs}$  is calculated by:

$$L_{fs} = \frac{\lambda_{rician}^2}{16\pi^2 \cdot L_{sys} \cdot d_{rician}^\alpha} \quad (12)$$

$L_{total}$  is calculated as:

$$L_{total} = R_r \cdot L_{fs} \quad (13)$$

$P_t$  is calculated as:

$$P_t = \frac{P_{rx}}{L} \quad (14)$$

The transmitter power is then set in the OBU.

The inverse fading model can be changed to use the Log-normal shadowing model [18], calculated as follows:

The mean path loss is calculated as:

$$L_{mean} = 10 \cdot \gamma \cdot \log_{10} \left( \frac{d}{d_0} \right) \quad (15)$$

the shadowing effect:

$$S \sim \mathcal{N}(0, \sigma_{dB}) \quad (16)$$

The total path loss ( $L_{total}$ ) is the sum of the mean path loss and the shadowing effect:

$$L_{total} = L_{mean} + S \quad (17)$$

The received power ( $P_{rx}$ ) is then converted to dBm. The required transmitter power ( $P_{tx}$ ) in dBm is determined by adding the received power in dBm and the total path loss:

$$P_{tx\_dBm} = P_{rx\_dBm} + L_{total} \quad (18)$$

The system was also extended with an SDR to replicate radio interference (transmitting gaussian noise). It utilized a simulation based probability density function (PDF) based on packet loss frequency data to generate the interfering signal frequency. The PDF was chosen with the help of the Kolmogorov-Smirnov test and found to be a log-normal distribution.

The system was exhaustively tested in a 70 minutes long proof of concept measurement campaign involving 3 real vehicles equipped with V2X devices moving on a  $\sim 10km$  long route in real traffic for five measurement cases with different radio settings.

The findings indicate that inverse fading models offer a more accurate depiction of communication between real and virtual vehicles than constant transmitter power configurations (see Table 6 and Table 7). The mesoscopic vehicle with its digital twin was able to move along with EGO vehicles, realizing the virtual traffic’s communication around them. The SDR radio was able to interfere with V2X hardware and provided realistic packet drops, losing up to 29.69% of sent messages.

Table 6: Summary of relative differences in RSSI average values of the inverse Rician Fading model and the Rician Fading model with a constant transmitter power compared to the received signal power of the simulation (the target receiver power levels in the physical domain).

| Case   | RSSI1 inverse model (%) | RSSI2 inverse model(%) | RSSI normal model(%) |
|--------|-------------------------|------------------------|----------------------|
| Case 1 | 18.57                   | 21.99                  | 76.98                |
| Case 2 | 25.70                   | 28.98                  | 80.72                |
| Case 3 | 27.41                   | 30.70                  | 80.33                |

Table 7: Summary of measurement cases with relative transmission power differences compared to the first measurement case.

| Case | RSSI1 Avg. [dBm] | RSSI2 Avg. [dBm] | Noise1 Avg. [dBm] | Noise2 Avg. [dBm] | Transmission Power Avg. [dBm] | Distance Avg. [m] | Relative Power Diff. [%] |
|------|------------------|------------------|-------------------|-------------------|-------------------------------|-------------------|--------------------------|
| 1    | -72.23           | -69.77           | -101.56           | -100.82           | 16.14                         | 202.38            | -                        |
| 2    | -47.00           | -41.00           | -101.00           | -104.00           | 11.71                         | 117.24            | -27.45%                  |
| 3    | -63.59           | -60.68           | -101.72           | -101.04           | 13.17                         | 127.81            | -18.38%                  |
| 4    | -59.05           | -56.18           | -101.65           | -100.98           | 7.76                          | 90.17             | -51.93%                  |
| 5    | -58.76           | -54.99           | -101.92           | -101.04           | 7.33                          | 123.38            | -54.58%                  |

# References

- [1] YL IEEE 802.11 p Working Group et al. “ISO/IEC/IEEE 8802-11:2022 Telecommunications and information exchange between systems — Specific requirements for local and metropolitan area networks — Part 11: Wireless LAN medium access control (MAC) and physical layer (PHY) specifications”. In: *IEEE Std* (2022).
- [2] Rafael Molina-Masegosa and Javier Gozalvez. “LTE-V for Sidelink 5G V2X Vehicular Communications: A New 5G Technology for Short-Range Vehicle-to-Everything Communications”. In: *IEEE Vehicular Technology Magazine* 12.4 (2017), pp. 30–39. DOI: [10.1109/MVT.2017.2752798](https://doi.org/10.1109/MVT.2017.2752798).
- [3] Othman S. Al-Heety et al. “Traffic Control Based on Integrated Kalman Filtering and Adaptive Quantized Q-Learning Framework for Internet of Vehicles”. In: *CMES - Computer Modeling in Engineering and Sciences* 138.3 (2023), pp. 2103–2127. ISSN: 1526-1492. DOI: <https://doi.org/10.32604/cmes.2023.029509>. URL: <https://www.sciencedirect.com/science/article/pii/S1526149223001480>.
- [4] Ziyi Lu et al. “Toward edge-computing-enabled collision-free scheduling management for autonomous vehicles at unsignalized intersections”. In: *Digital Communications and Networks* (2024). ISSN: 2352-8648. DOI: <https://doi.org/10.1016/j.dcan.2024.03.001>. URL: <https://www.sciencedirect.com/science/article/pii/S2352864824000270>.
- [5] Dekai Zhu, Qadeer Khan, and Daniel Cremers. “Multi-vehicle trajectory prediction and control at intersections using state and intention information”. In: *Neurocomputing* 574 (2024), p. 127220. ISSN: 0925-2312. DOI: <https://doi.org/10.1016/j.neucom.2023.127220>. URL: <https://www.sciencedirect.com/science/article/pii/S0925231223013437>.
- [6] Snigdhaswin Kar, Prabodh Mishra, and Kuang-Ching Wang. “Dynamic packet duplication for reliable low latency communication under mobility in 5G NR-DC networks”. In: *Computer Networks* 234 (2023), p. 109923. ISSN: 1389-1286. DOI: <https://doi.org/10.1016/j.comnet.2023.109923>. URL: <https://www.sciencedirect.com/science/article/pii/S1389128623003687>.

- [7] Vittorio Todisco et al. “Full duplex based collision detection to enhance the V2X sidelink autonomous mode”. In: *Computer Networks* 254 (2024), p. 110763. ISSN: 1389-1286. DOI: <https://doi.org/10.1016/j.comnet.2024.110763>. URL: <https://www.sciencedirect.com/science/article/pii/S1389128624005954>.
- [8] Hieu Nguyen et al. “Cellular V2X Communications in the Presence of Big Vehicle Shadowing: Performance Analysis and Mitigation”. In: *IEEE Transactions on Vehicular Technology* (2022), pp. 1–13. DOI: 10.1109/TVT.2022.3212704.
- [9] Behrad Toghi et al. “Analysis of Distributed Congestion Control in Cellular Vehicle-to-Everything Networks”. In: *2019 IEEE 90th Vehicular Technology Conference (VTC2019-Fall)*. 2019, pp. 1–7. DOI: 10.1109/VTCFall.2019.8891335.
- [10] Weiming Zhao, Ronghui Liu, and Dong Ngoduy. “A bilevel programming model for autonomous intersection control and trajectory planning”. In: *Transportmetrica A: transport science* 17.1 (2021), pp. 34–58.
- [11] Yang Guan et al. “Centralized Cooperation for Connected and Automated Vehicles at Intersections by Proximal Policy Optimization”. In: *IEEE Transactions on Vehicular Technology* 69.11 (2020), pp. 12597–12608. DOI: 10.1109/TVT.2020.3026111.
- [12] Chairit Wuthishuwong and Ansgar Traechtler. “Coordination of multiple autonomous intersections by using local neighborhood information”. In: *2013 International Conference on Connected Vehicles and Expo (ICCVE)*. 2013, pp. 48–53. DOI: 10.1109/ICCVE.2013.6799768.
- [13] John Khoury, Joud Khoury, and Germain Zouein. “A practical approach to decentralized intersection access control for autonomous vehicles”. In: *Proceedings of the 2017 International Conference on Automation, Control and Robots*. 2017, pp. 32–35.
- [14] Alexander Katriniok, Peter Kleibaum, and Martina Joševski. “Distributed Model Predictive Control for Intersection Automation Using a Parallelized Optimization Approach”. In: *IFAC-PapersOnLine* 50.1 (2017). 20th IFAC World Congress, pp. 5940–5946. ISSN: 2405-8963. DOI: <https://doi.org/10.1016/j.ifacol.2017.08.1492>. URL: <https://www.sciencedirect.com/science/article/pii/S2405896317320694>.
- [15] Laleh Makarem and Denis Gillet. “Fluent coordination of autonomous vehicles at intersections”. In: *2012 IEEE International Conference on Systems, Man, and Cybernetics (SMC)*. 2012, pp. 2557–2562. DOI: 10.1109/ICSMC.2012.6378130.
- [16] ETSI Technical Committee Intelligent Transport Systems. *Intelligent Transport Systems (ITS); Vehicular Communications; Basic Set of Applications; Part 2: Specification of Cooperative Awareness Basic Service*. en. Standard ETSI EN 302 637-2. Sophia-Antipolis, France: European Telecommunications Standards Institute, 2019.

- URL: [https://www.etsi.org/deliver/etsi\\_EN/302600\\_302699/30263702/01.04.01\\_30/en\\_30263702v010401v.pdf](https://www.etsi.org/deliver/etsi_EN/302600_302699/30263702/01.04.01_30/en_30263702v010401v.pdf).
- [17] Chengshan Xiao, Yahong Rosa Zheng, and Norman C Beaulieu. “Statistical simulation models for Rayleigh and Rician fading”. In: *IEEE International Conference on Communications, 2003. ICC’03*. Vol. 5. IEEE. 2003, pp. 3524–3529.
- [18] Charalambos D Charalambous and Nickie Menemenlis. “Dynamical spatial log-normal shadowing models for mobile communications”. In: *Proceedings of the 27th General Assembly of the International Union of Radio Science* (2002).

# Publications of the Author

- [A] T. Ormándi and B. Varga, *The importance of V2X simulation: An in-depth comparison of intersection control algorithms using a high-fidelity communication simulation*, Vehicular Communications, vol. 44, p. 100676, 2023. Elsevier. Available: <https://doi.org/10.1016/j.vehcom.2023.100676>.
- [B] T. Ormándi, B. Varga, and T. Tettamanti, *Distributed intersection control based on cooperative awareness messages*, 2021 5th International Conference on Control and Fault-Tolerant Systems (SysTol), IEEE, 2021. Available: <https://doi.org/10.1109/SysTol52990.2021.9595376>.
- [C] T. Wágner, et al., *SPaT/MAP V2X communication between traffic light and vehicles and a realization with digital twin*, Computers and Electrical Engineering, vol. 106, p. 108560, 2023. Elsevier. Available: <https://doi.org/10.1016/j.compeleceng.2022.108560>.
- [D] M. Novák, B. Varga, T. Ormándi, *Analysis of Safety and Security in Autonomous Intersections*, 2025 11th International Conference on Control, Decision and Information Technologies (CoDIT), IEEE, 2025. (Submitted)
- [E] T. Ormándi, B. Varga, *Mesoscopic V2X Simulation Framework to Enhance Simulation Performance*, Simulation Modelling Practice and Theory, 2024. Available: <https://doi.org/10.1016/j.simpat.2024.103003>.
- [F] B. Varga, T. Ormándi, T. Tettamanti, *EGO-centric, multi-scale co-simulation to tackle large urban traffic scenarios*, IEEE Access, 2023. Available: <https://doi.org/10.1109/ACCESS.2023.3284316>.
- [G] T. Ormándi, B. Varga, *Proof of concept testing of a mixed-reality VANET test system with SDR-based physical radio interference*, 23rd European Control Conference (ECC25), 2025. (Accepted)
- [H] T. Ormándi, B. Varga, *V2X link-based Digital Twins with inverse fading model for mixed-reality testing of CCAM functions*, IEEE Transactions on Intelligent Vehicles, 2025. (Submitted)

- [I] T. Ormándi, Zs. Pethő, B. Varga, *Mixed-reality VANET testing supported by simulation of mesoscopic V2X communication*, 2024 10th International Conference on Control, Decision and Information Technologies (CoDIT), IEEE, 2024, pp. 1915–1920. Available: <https://doi.org/10.1109/CoDIT62066.2024.10708241>.
- [J] T. Ormándi, *Practical Manual of SUMO/MATLAB/VEINS/INET/OMNET++ PROGRAMMING AND INTERFACING for V2X Simulation with Standard Protocols (Technical Report)*. Available: [https://traffic.bme.hu/wp-content/uploads/2023/02/Veins\\_Documentation.pdf](https://traffic.bme.hu/wp-content/uploads/2023/02/Veins_Documentation.pdf).